Published in final edited form as:
Neuroimage. 2010 October 1; 52(4): 1495–1504. doi:10.1016/j.neuroimage.2010.05.011.

A study of the reproducibility and etiology of diffusion anisotropy differences in developmental stuttering: a potential role for impaired myelination

M.D. Cykowski[1], **P.T. Fox**[1,2,3,4,6], **R.J. Ingham**[1,5], **J.C. Ingham**[1,5], and **D.A. Robin**[1,3,4,6]

[1]Research Imaging Center, University of Texas Health Science Center at San Antonio, San Antonio, TX 78284, USA

[2]VA Medical Center, San Antonio, TX 78229, USA

[3]Department of Radiology, University of Texas Health Science Center at San Antonio

[4]Department of Neurology, University of Texas Health Science Center at San Antonio

[5]Department of Speech and Hearing Sciences, University of California, Santa Barbara, CA 93106, USA

[6]University of Texas at San Antonio, San Antonio, TX, 78249, USA

Abstract

Several diffusion tensor imaging (DTI) studies have reported fractional anisotropy (FA) reductions within the left perisylvian white matter (WM) of persistent developmental stutterers (PSs). However, these studies have not reached the same conclusions in regard to the presence, spatial distribution (focal/ diffuse), and directionality (elevated/reduced) of FA differences outside of the left perisylvian region. In addition, supplemental DTI measures (axial and radial diffusivities, diffusion trace) have yet to be utilized to examine the potential etiology of these FA reductions. Therefore, the present study sought to reexamine earlier findings through a sex- and age-controlled replication analysis and then to extend these findings with the aforementioned non-FA measures. The replication analysis showed that robust FA reductions in PSs were largely focal, left hemispheric, and within late-myelinating associative and commissural fibers (division III of the left superior longitudinal fasciculus, callosal body, forceps minor of the corpus callosum). Additional DTI measures revealed that these FA reductions were attributable to an increase in diffusion perpendicular to the affected fiber tracts (elevated radial diffusivity). These findings suggest a hypothesis that will be testable in future studies: that myelogenesis may be abnormal in PSs within left-hemispheric fiber tracts that begin a prolonged course of myelination in the first postnatal year.

Corresponding author: Matthew D. Cykowski, M.D., Institution: Research Imaging Center, University of Texas Health Science Center at San Antonio, San Antonio, TX 78284, cykowski@uthscsa.edu, Phone: (210) 567-8169; Fax: (210) 567-8152.

Keywords

developmental stuttering; radial diffusivity; myelogenesis; superior longitudinal fasciculus; dysmyelination

Persistent developmental stuttering (PS) is a speech disorder characterized by the involuntary repetition and/ or prolongation of sounds and syllables (Wingate, 1964). These audible and silent speech events are often accompanied by variable signs of “speech-related struggle” (Wingate, 1964) (p. 488), such as involuntary movements of the eyes, head, tongue, and lips (Bloodstein and Ratner, 2008). More proximal events in speech production are also thought to be abnormal in developmental stuttering, including atypical laryngeal movement during stuttered speech (Conture et al., 1977) and relatively slow initiation and termination of phonation (Adams and Hayden, 1976). Persistent developmental stutterers (PSs) have also been found to differ in the performance of simple non-speech bimanual tasks (Webster, 1993), and kinematic analyses of non-speech orofacial and finger movements have found evidence for “generalized neuromotor differences” in PSs (p. 228) (Max et al., 2003). Given these differences in speech and non-speech behaviors it is not surprising that a central nervous system origin for the disorder was advanced as early as the 1920s (Orton, 1927). Recent functional neuroimaging studies have confirmed this early hypothesis by repeatedly demonstrating atypical patterns of cerebral activity during stuttered speech (De Nil et al., 2000; Fox et al., 1996; Wu et al., 1995), as well as during fluent speech (Stager et al., 2003) and non-speech behaviors of PSs (Braun et al., 1997; Chang et al., 2009; Ingham et al., 2000). It is currently less clear whether underlying neuroanatomical abnormalities might help to explain the pervasive neurophysiological differences underlying stuttered speech production (Ingham et al., 2007).

The structural neuroimaging studies that have been performed with PSs and matched controls can be broadly divided into investigations of pre- or postnatal brain development. This division is based on the neurodevelopmental events reflected in the anatomical features under consideration (sulcal formation versus myelination in associative fibers). Studies utilizing metrics of prenatal brain development (in adult PSs and children who stutter) have considered their sulcal and gyral anatomy, cerebral asymmetry, and/ or cortical anatomy (Beal et al., 2007; Chang et al., 2008; Cykowski et al., 2008; Foundas et al., 2001; Foundas et al., 2003). The metrics used in these studies of PS ultimately reflect prenatal neurodevelopmental events including neuronal migration and cortical lamination, the asymmetric growth of homologous structures (e.g., planum temporale), and the attainment of adult-like gyrification and sulcal patterns (Armstrong et al., 1995; Galaburda et al., 1978; Sidman and Rakic, 1973). In brief, these studies of PS have produced inconsistent results in regard to the presence of atypical cerebral asymmetry (Chang et al., 2008; Cykowski et al., 2008; Foundas et al., 2001; Foundas et al., 2003), cortical anatomy (Beal et al., 2007; Chang et al., 2008; Jancke et al., 2004), and gyrification patterns (Cykowski et al., 2008; Foundas et al., 2001). Given these inconsistencies it is unclear whether gross anatomical features that arise largely during prenatal brain development are different between PSs and normally fluent speakers (NSs).

The second category of anatomical studies in PS has characterized the microstructural features of white matter (WM) in both children (Chang et al., 2008) and adults who stutter (Sommer et al., 2002; Watkins et al., 2008). All of these studies have utilized diffusion tensor imaging (DTI) to examine the anisotropy of water molecule diffusion within WM tracts (Basser and Jones, 2002). The first of these DTI studies by Sommer and colleagues identified a single, focal reduction of FA in the left perisylvian WM of PSs near the left rolandic operculum (Sommer et al., 2002). Subsequent DTI studies confirmed an FA reduction in this region (Chang et al., 2008; Watkins et al., 2008). In addition, Watkins and colleagues also identified a more diffuse and bilateral pattern of FA reduction (Watkins et al., 2008), suggesting a non-focal pathophysiologic process underlying reduced diffusion anisotropy in PSs. Chang and colleagues, studying children who stutter, identified predominantly left-sided FA reductions in the area of the superior longitudinal fasciculus, as well as bilateral findings in the corticospinal tracts (Chang et al., 2008). Further, both of these latter studies identified areas wherein FA values were significantly higher in PSs than fluent speakers. These differences among studies might have reflected differences in the PSs participating, the stringent but uncorrected statistical thresholds of the later studies (Chang et al., 2008; Watkins et al., 2008), or possibly a far more extensive WM abnormality than just the tracts of the left perisylvian region (Sommer et al., 2002). Nonetheless, the consistent finding of a reduction in the FA of left perisylvian WM is notable as the fiber tracts in this region myelinate entirely in the postnatal period (Yakovlev and Lecours, 1967). Indeed, the cerebral WM fiber tracts that have been the target of investigations in PS do not demonstrate signs of early myelination until the 40^{th} week of gestation (e.g., the visual system). Many of these tracts continue to myelinate during the first postnatal year and complete myelination in the second year (e.g., corticospinal projection fibers) (Kinney et al., 1988), though some continue to myelinate past the first decade of life (Yakovlev and Lecours, 1967).

The present study was designed as a replication and extension analysis relative to the second category of neuroanatomical studies in PS (the study of WM microstructure). For the replication aspect of the study, a voxelwise analysis was performed with DTI data from 13 male PSs and 14 sex- and age-matched controls using the Tract Based Spatial Statistics (TBSS) approach (Smith et al., 2006). To increase the reliability of the replication analysis, a robust algorithm for DTI preprocessing was utilized that accounts for outlier data points in diffusion-weighted imaging data (Chang et al., 2005). To increase the specificity of the analysis, a threshold-free cluster enhancement (TFCE) method of multiple comparison correction was implemented (Smith and Nichols, 2009). As an important extension of prior analyses, this study then examined three supplemental DTI parameters to elucidate the potential bases of FA reductions within the affected WM tracts of PSs. These measures included the trace of the diffusion tensor (Tr (D)), representing the orientation-independent averaged molecular displacement of water molecules within tissue (Le Bihan et al., 2001). The measures also included axial ($\lambda_{\parallel}$) and radial diffusivity ($\lambda_{\perp}$), which represent the diffusion parallel to the long axis of fibers and the average diffusion perpendicular to the long axis of fibers, respectively (Budde et al., 2008). These supplemental parameters allowed for a more complete characterization of the potential etiology of WM differences (Budde et al., 2008; Song et al., 2002; Song et al., 2005) in PSs. This step is crucial as FA reductions can follow a variety of unrelated pathological processes such as WM

degeneration following ischemic stroke (Thomalla et al., 2005), progressive demyelinating disease (Vrenken et al., 2006), developmental dysmyelination (Guo et al., 2001), and axonal damage (DeBoy et al., 2007). In summary, this study aimed to further characterize the most robust neuroanatomical effects of interest in PSs and then determine their potential pathophysiological bases using secondary DTI parameters (Tr (D), $\lambda_{\|}$, $\lambda_{\perp}$). This study should assist future investigations that aim to examine postnatal WM development in these particular regions in relation to the onset, persistence, and recovery from stuttering, especially in children.

MATERIALS AND METHODS

Subjects

Both persistent developmental stuttering speakers (PSs) (n = 13) and normally fluent speakers (NSs) (n = 14) participated in the study. All subjects were male and matched for age, handedness (Oldfield, 1971), and years of education (see Table 1), and all subjects were native English speakers. Both PSs and NSs were excluded if they had any history of brain and/ or other central nervous system surgery, head trauma, endocrine disorders, seizure disorder, stroke, major depressive disorder or anxiety disorder, schizophrenia, substance abuse, attention deficit disorder, history of speech and/ or developmental neurological abnormalities aside from PS, hypertension, and hyperlipidemia. Three PSs and 3 NS were excluded from this study on these grounds after reviewing all available records on the participants, including their intake medical history questionnaires, prior records from unrelated studies, or as obtained on follow-up interview (leaving the final numbers of 14 NS and 13 PSs). Imaging was performed at the Research Imaging Center with the informed written consent of the participants and the approval of the University of Texas Health Science Center at San Antonio Institutional Review Board.

Speech history and speech assessment

PSs self-reported a diagnosis of PS prior to the age of 8 years and were confirmed to stutter during expert-judged 3-minute audiovisual recordings of oral reading, spontaneous monologue, and telephone conversation tasks. Stuttering behavior in PSs was assessed as the percentage of syllables stuttered (Ingham et al., 1999). Control subjects reported no history of stuttering, other speech disorders, or hearing disorders. Their fluency was assessed using the same 3-minute oral reading, phone, and monologue assessments as used in PSs. These audiovisual recordings were also reviewed by independent judges (University of California – Santa Barbara and the University of Georgia), blind to subject grouping and expert in the evaluation of PSs. Both sets of judges agreed that these control subjects were fluent speakers who did not have any events of stuttered speech.

MRI acquisition

DTI acquisitions were done using a 3-Tesla Siemens Trio scanner and an eight-channel head coil (Kochunov et al., 2007). Briefly, a single-shot, spin-echo EPI sequence (TR/ TE = 10100 / 89 ms; NSA = 1; 5/8 partial Fourier encoding) was used to obtain two-dimensional diffusion-weighted images covering the entire brain without any gaps (array size: 128 × 128 × 65; in-plane resolution = 1.72 × 1.72 mm; slice thickness = 2.0 mm). Three reference

images were acquired without diffusion weighting (*b*-value = 0) and 86 images were acquired using isotropically distributed diffusion weighted directions (*b*-value = 700 sec / mm^2). This sequence has been reported previously (Kochunov et al., 2010) and the number of diffusion directions, b0 images, and the *b*-value were calculated using an optimization technique that accounts for the diffusivity of cerebral WM and T2 relaxation times (Jones et al., 1999). The acquisition time per subject was approximately 15 minutes.

Image preprocessing

Diffusion-weighted images were concatenated into a four-dimensional file (89 time points) that matched the order of the *b*-values and normalized gradient vectors applied during the imaging session. The data were corrected for eddy current artifacts, the geometric image distortions resulting from rapidly switching gradient fields (Basser and Jones, 2002), by using the FMRIB software library (FSL) tool FLIRT (Jenkinson et al., 2002). FLIRT was then used to register the diffusion-weighted images to a non-diffusion weighted reference volume using a mutual information cost function for 12-parameter affine registration. Aligned volumes were resliced with sinc interpolation, the three reference images without diffusion weighting were averaged, and a mask of the brain was generated from the T2 average using the FSL program Brain Extraction Tool (BET) (Smith et al., 2004). Each volume in the aligned, four-dimensional data was multiplied by the binary mask of the average reference volume to remove nonbrain tissues.

Diffusion tensor fitting with RESTORE algorithm

Subsequent image processing steps were done with the Camino Diffusion MRI Toolkit (Cook et al., 2006). The diffusion tensor was fit at each voxel per subject using the “Robust Estimation of Tensors by Outlier Rejection” (RESTORE) algorithm (Chang et al., 2005), as implemented in Camino. The RESTORE algorithm utilizes nonlinear least-square (NLS) regression and incorporates several cycles of iteratively reweighted NLS regression to identify and remove data outliers prior to a final NLS tensor fit (Chang et al., 2005). This approach offers a number of advantages over standard linear least squares fitting methods, including the removal of artifacts due to cardiac pulsation from ungated acquisitions, as well as those due to subject motion (Chang et al., 2005).

Generation of scalar measurements for statistical analyses

Following tensor fitting, images of the following scalar measurements were generated: fractional anisotropy (FA), trace of the diffusion tensor (Tr (D)), and the first (λ_1), second (λ_2), and third (λ_3) eigenvalues. The first eigenvalue (λ_1) is assumed to represent diffusion processes parallel to the axons within WM tracts (Song et al., 2005), and is hereafter referred to as “axial diffusivity” ($\lambda_{||}$). Likewise, the average of the second and third eigenvalues, representing the diffusion processes perpendicular to the long axis of axons (Song et al., 2005), is hereafter referred to as “radial diffusivity” ($\lambda_{\perp}$).

Tract-based spatial statistics (TBSS)

Voxelwise statistical analyses of scalar parameter images (e.g., FA images) were carried out in the program Tract-based spatial statistics (TBSS) (Smith et al., 2006). Within routine

TBSS processing, the FA images were aligned to a high-resolution standard-space FA image (www.fmrib.ox.ac.uk/fsl/tbss/FMRIB58_FA), using the FSL program FNIRT (www.fmrib.ox.ac.uk/fsl/fnirt/index.html). The subject FA images were resliced to an isotropic resolution of 1 mm through this registration step. A mean FA image was created by averaging the aligned individual FA images and was subsequently thinned to create a voxel-thick skeleton of the center of major WM fiber tracts (a “mean FA skeleton”) (Smith et al., 2006). The mean FA skeleton was thresholded at FA = 0.2 to ensure that the skeleton did not include non-WM tissues (e.g., cortex). Subject-specific FA skeleton images were generated by projecting nearby maximum FA values onto the invariant mean FA skeleton. A ‘distance map’ was used to ensure that FA values were projected onto the nearest mean FA skeleton surface and a Gaussian weighting function was used to weight FA values near the mean FA skeleton more heavily (Smith et al., 2006). The nonlinear warps, skeleton projection, and projection vectors from TBSS processing of FA images were then applied to the three sets of non-FA images (Tr (D), λ_1, $\lambda_{||}$).

Statistical analyses

Whole brain, cross-subject voxelwise statistics were performed using the general linear model as implemented in the FSL program Randomise. This was used to implement a two-group, unpaired t-test to compare FA between PSs and NSs, while treating mean percentage of syllables stuttered as a covariate of interest within the PSs. The mean percentage of syllables stuttered per subject was computed as the average agreement between judges for percentage syllables stuttered across monologue, reading, and telephone speaking tasks (see Appendix 1 for rationale). Each speaking task was rated by two, independent judges (interrater agreement of $r = 0.984$, $p \leq 0.05$, $v = 37$).

Inferences on the raw statistic images were performed using the permutation method implemented in the Randomise program (Nichols and Holmes, 2002). The corrected data was thresholded using both one-tailed testing (corrected, one-tailed $p \leq 0.03$) and two-tailed testing (corrected, two-tailed $p \leq 0.05$) following the TFCE algorithm (Smith and Nichols, 2009). One-tailed testing was performed on these corrected results to increase study sensitivity, particularly as multiple studies have now described reduced anisotropy in PSs relative to NSs (Chang et al., 2008; Sommer et al., 2002; Watkins et al., 2008). Likewise, two-tailed testing was performed on the corrected results to determine which regions, if any, demonstrated the most robust FA reductions. Additional statistical analyses utilizing the non-FA parameters are described below (see “Significant differences in DTI parameters between PSs and NSs”).

RESULTS

Subject characteristics and speech assessments

The mean values and standard deviations for age, handedness, education, and percentage syllables stuttered are shown in Table 1 (see footnotes for additional detail).

Significant differences in DTI parameters between PSs and NSs

Figure 1 demonstrates the voxels where FA values of PSs were significantly lower than those of fluent speakers. The labels shown in Figure 1 were assigned using the MNI space ICBM DTI-81 atlas (Mori et al., 2008), a histological atlas (Schmahmann and Pandya, 2006), and recent DTI studies of the superior longitudinal fasciculus (Makris et al., 2005).

The one-tailed, corrected results ($p \leq 0.03$) encompassed two large clusters (Table 2) where the FA values of PSs were significantly lower than NSs. The first of these included a continuous region of WM from the left forceps minor near its junction with the left anterior corona radiata, extending dorsally and caudally through the third division of the left superior longitudinal fasciculus (including WM deep to Brodmann area (BA) 44). The second of these clusters included WM within the body of the corpus callosum. In contrast, there were no regions where the FA values of PSs were significantly greater than those of NSs.

The two-tailed, corrected results ($p \leq 0,05$) demonstrate a more limited set of WM regions within those described above where the FA values of PSs were significantly lower than NSs. Specifically, these findings were limited to the superior longitudinal fasciculus (Figure 1, z = 21) extending rostromedially into the left anterior corona radiata and left forceps minor. As described above, there were no regions where the FA values of PSs were significantly greater than those of NSs.

To increase the sensitivity to FA differences, Table 2 focuses on one-tailed, corrected results (Figure 1), as FA reductions in PSs have now been seen across three prior studies (Chang et al., 2008; Sommer et al., 2002; Watkins et al., 2008). Table 2 lists the features of two large clusters in these results, including the fiber tracts encompassed, their size, the MNI and Talairach coordinates of the centroids, and the mean values and standard deviations of all DTI parameters studied (FA, Tr (D), $\lambda_{\perp}$, and $\lambda_{\parallel}$). The mean and standard deviation of the non-FA parameters shown in Table 2 were obtained by creating a mask of the WM regions demonstrated in Figure 1 (one mask for each of the two clusters in the one-tailed, corrected results).

A Mann-Whitney U test was performed as a posthoc comparison of the regional mean values of Tr (D), $\lambda_{\perp}$, and $\lambda_{\parallel}$. Radial diffusivity was significantly elevated in PSs (at the Bonferroni-corrected p value of 0.0083) for the tracts of both clusters. Likewise, Tr (D) was significantly elevated in PSs within the second cluster (the callosal body). The comparisons of Tr (D) for the first cluster (encompassing the left superior longitudinal fasciculus, anterior corona radiata, and forceps minor) and $\lambda_{\parallel}$ were not significant at the corrected p-value.

Relationship between fractional anisotropy and stuttering frequency

No significant relationship was detected between the FA measures in PSs and the mean percentage of syllables stuttered.

Post-hoc quality assurance steps for the statistical comparison of eigenvalues

Wheeler-Kingshott and Cercignani (2009) recently highlighted potential problems in comparing the major and minor eigenvalues, from which $\lambda_{\parallel}$ and $\lambda_{\perp}$ are determined, respectively. Specifically, that work demonstrated that in areas of low anisotropy (gray

matter, voxels with partial voluming, and crossing fiber tracts), the orientation of the principal eigenvector might differ substantially across subjects (> 45°). In these cases the eigenvalues across subjects no longer reflect the same underlying tissue architecture.

To address this in the present study, a post-hoc quality assurance step (see Appendix 2) was designed to examine whether our statistical comparisons of $\lambda_{\parallel}$ and $\lambda_{\perp}$ were confounded by these issues. Briefly, the aim of this step was to determine the variability of principal eigenvector orientation across subjects (in degrees) from the group median principal eigenvector. This analysis was performed for an area of the results that would be the most susceptible to the confounds discussed by Wheeler-Kingshott and Cercignani (2009) within a region-of-interest closest to the findings of Sommer et al. (2002). Using this method for the native space diffusion tensor eigensystem of each subject, the average voxelwise deviation from the group median eigenvector was determined to be 17.8° (sd = 3.2) and a two-tailed t-test demonstrated no significant differences in the angle of deviation between controls and stutterers ($t = 0.79$, $p = 0.43$). These results confirmed the present DTI data were suitable for minor eigenvalue comparisons.

It is likely that the deviation of the principal eigenvector orientation across subjects was relatively small for two reasons. First, the areas of significant difference in the present study that were examined in this posthoc step were in areas of relatively high anisotropy (Table 2), not lower anisotropy as would be expected in voxels of gray matter or those with a substantial partial voluming effect. Second, the TBSS method ensures that the white matter voxels analyzed conform to the center of highly directional and anisotropic fiber tracts (e.g., corpus callosum, superior longitudinal fasciculus).

DISCUSSION

This investigation sought to further characterize the spatial distribution of the most robust FA reductions in PSs and then to extend the current understanding of these reductions through the use of supplemental DTI parameters. As in prior DTI studies of PS (Chang et al., 2008; Sommer et al., 2002; Watkins et al., 2008), the replication portion of the analysis revealed FA reductions in PSs, with particular overlap seen in the left, ventral perisylvian WM (Figure 2). Supplemental DTI measures revealed that these FA reductions in PSs were strongly influenced by increased radial diffusivity, representing diffusion perpendicular to the main fiber orientation. A similar combination of FA reduction with elevated radial diffusivity has been seen in dysmyelination (the improper formation of the myelin sheath during brain development) (Song et al., 2002). In addition, the significant elevation of Tr (D) observed in PSs within the callosal body, as well as the non-significant elevation in the first WM cluster, may be related to the elevation of radial diffusivity and thus offer additional evidence for a myelination abnormality. Specifically, the mean diffusivity of tracts (equal to one-third of the Tr (D)) can be significantly elevated in dysmyelination, even when radial diffusivity is the more sensitive marker (Harsan et al., 2007). Altogether, these findings can tentatively be interpreted as evidence that myelogenesis is impaired in the WM of PSs. The tracts in which the process of myelogenesis appears to be affected are those that do not even initiate myelination until approximately 4–6 postnatal months (Kinney et al., 1988; Yakovlev and Lecours, 1967).

A comparison of DTI findings across studies

As demonstrated in Figure 2, there is evidence among studies of PS for the spatial overlap of FA reductions in the left ventral frontal lobe and rolandic operculum WM (see sagittal slices of Figure 2 at x = −39 and −45 and axial slices at z = 23, 18, and 13). The consistency of this finding using a low resolution, "artifact-prone" technique (Mori, 2002, p. 392) is remarkable, as this technical limitation is compounded with disparities in subject characteristics and DTI acquisition protocols among studies of PSs (Chang et al., 2008; Sommer et al., 2002; Watkins et al., 2008). The most robust and tract-specific finding is that each of these DTI studies of PSs has found WM abnormalities within the ventral subdivision of the superior longitudinal fasciculus (see sagittal slices of Figure 2). Likewise, a recent report by Kell and colleagues compared the data of recovered and persistent stutterers to NS. That study also found FA reductions within the left perisylvian WM, but these reductions did not exceed the corrected significance threshold (Kell et al., 2009).

The portion of the superior longitudinal fasciculus wherein these robust findings have been seen is deep to the perisylvian postcentral, central, and frontal opercula (deep to Brodmann area (BA) 44). Specifically, this tract has been termed the third division of the superior longitudinal fasciculus (SLF III) (Makris et al., 2005), a distinctly different entity than the more medially- and dorsally-located arcuate fasciculus (which runs with SLF II fibers). This tract-specific distinction is critical because the SLF III contains bidirectional connections between speech-relevant areas of the ventral premotor cortex/ BA 44 and secondary somatosensory areas in the inferior parietal lobule (Makris et al., 2005) (see "Implications of robust DTI findings for stuttered speech production" below).

Several results here did not overlap with the results of prior studies. As shown in Figure 2, recent studies have demonstrated a more widespread pattern of decreased WM integrity than was seen in the original DTI report (Sommer et al., 2002). It should be noted among the studies demonstrated in Table 2 that not all included analyses within the brainstem and cerebellar white matter (the present study did include these areas). The present results did not reveal a diffuse and bilateral reduction in FA, but rather a more focal and predominantly left-hemispheric distribution of affected tracts (with FA reductions also observed in the corpus callosum using a one-tailed correction). A plausible reason for this difference is the slightly more stringent statistical threshold applied here to enhance finding specificity. Possibly for the same reason, no regions of significantly elevated FA in PSs (relative to fluent speakers) were observed in the present study.

The FA reductions observed in the corpus callosum of PSs were also largely attributable to an increase in $\lambda_{\perp}$. It is not clear as yet whether these findings are group-or PSs-specific, as they do not have precedent in any prior study of PSs (see Figure 2 at z = 28). It may be that this finding is the result of restricting the present analysis to adult male participants and that these FA reductions are worthy of investigation for potential replication in independent samples. However, there is also a possibility these reductions are sample-specific, similar to the study-specific findings in PSs seen with prior studies (Figure 2). If replicated, this loss of white matter integrity in the corpus callosum might relate to a variety of experimental studies suggesting atypical interhemispheric coordination of excitatory and inhibitory signals (Greiner et al., 1986). Sommer and colleagues (2009) recently tested this relationship

and actually found that interhemispheric inhibition for the bilateral motor cortices of PSs was normal and not atypical. Further complicating the current understanding of the role of the corpus callosum and interhemispheric signaling during stuttered speech are conflicting functional neuroimaging results that suggest speech-related right hemispheric activity in PSs is compensatory in nature (Braun et al., 1997), versus related directly to stuttering behavior itself (Fox et al., 1996). Future studies of PSs that combine modalities might be able to further comment on these particular findings in innovative parametric designs (the relationship of callosal diffusion anisotropy and TMS measures of transcallosal inhibition).

Implications of robust DTI findings for stuttered speech production

In considering the differences observed in the SLF III of PSs (see Figure 2 at x = −39), the Directions Into Velocities of Articulators (DIVA) neural model of speech (Guenther et al., 2006) and “dual stream model” of speech processing (Hickok and Poeppel, 2007) provide explanatory power, albeit with different implications. We restrict our discussion to those components that require a connection between inferior parietal and ventral frontal cortices, because the fiber connections between these sites are subserved by the third division of the superior longitudinal fasciculus (SLF III) (Makris et al., 2005), where FA differences were observed in the present study.

The DIVA model suggests that the lateral ventral frontal cortex subserved by SLF III contains a ‘speech sound’ map, whose neurons encode the sounds to be produced by articulators. Likewise, the DIVA model proposes that the left inferior parietal cortex, both projecting to and receiving projections from the ventral frontal cortex contains both ‘somatosensory state’ and ‘somatosensory error’ maps, encoding the somatic sensations associated with syllable production and the discrepancy between intended and perceived speech actions, respectively. As mentioned above, the connections between the cortical regions where the DIVA model speech sound and somatosensory error maps are located are effectively via the SLF III (Makris et al., 2005). This is of functional importance in normal speech development since the model indicates this pathway is used to transmit somatosensory error signals to the ventral premotor cortex through corrective motor commands (p. 282) (Guenther et al., 2006). Within the DIVA framework, the present results would point to an imbalance between motor speech planning and somatosensory error monitoring due to the impaired myelogenesis of the left SLF III.

A second model that holds different implications for these results is the “dual-stream model” of speech processing. In the model, a ventral stream is involved in processing speech sounds for comprehension and a dorsal stream is “involved in translating acoustic speech signals into articulatory representations in the frontal lobe” (p. 394) (Hickok and Poeppel, 2007). Of relevance to the present results, the dorsal stream is proposed to be more left-hemisphere dominant, and as referenced in the DIVA model above, includes connections between the inferior parietal lobe/ operculum and the frontal cortex (e.g., via the SLF III observed here). This stream serves an “auditory-motor integration” role (p. 394) that is particularly important when speech requires more sensory guidance: with novel, low frequency, and more complex words (p. 400) (Hickok and Poeppel, 2007). If this process were dysfunctional in PS then one would anticipate that stuttering behavior would occur more

frequently with increased requirements on speech processing subserved by the dorsal stream (e.g., with low-frequency and/ or novel words). Notably, this is a prominent feature of stuttering behavior (Bloodstein and Ratner, 2008). It is important to recognize that the concept of an impaired utilization of auditory feedback for speech motor control by PSs is not novel (Yates, 1963) and the resolution of this dysfunction has been proposed as the mechanism underlying “fluency-inducing procedures” in PS (chorus reading, etc.) (Stager et al., 2003). The addition to this model that might be made by this study is that suboptimal auditory-motor integration in PSs may be the product of an altered course of postnatal myelogenesis in the left SLF III.

The concept of a *dysfunctional connection* between left inferior parietal lobule and ventral frontal lobe is consistent with the idea that stuttering arises from some atypical interaction among several functional areas involved in rapid speech production (Ludlow and Loucks, 2003). Thus, it is important to emphasize that these DTI findings are conceptualized as a dysfunctional but intact connection between speech-related areas, and not as complete disconnections between areas. For example, the FA values within the SLF III WM in the PS group still remain relatively high (see Table 2) compared to many WM and non-WM regions (e.g., cortex), even if significantly lower than that expected in NSs (Figure 1). This is important evidence for some degree of WM integrity in the affected regions of PSs (also confirmed by the normal axial diffusivity measurements at these sites). That these findings represent a dysfunctional but intact connection between speech areas is consistent with the variable appearance of both stuttering and fluent episodes in the speech of PSs, often dependent on the speaking situation (Bloodstein and Ratner, 2008), rather than a permanent speech deficit as might be expected from frank tissue damage. This also makes the present results difficult to interpret in terms of acquired speech disorders that would arise from ischemic tissue necrosis in the SLF WM fibers and surrounding cortex (Benson and Ardila, 1996). Specifically, if the overlap in DTI studies and present results suggest impaired postnatal myelogenesis in the SLF III of PSs, it would be difficult to make any meaningful analogy between this developmental phenomenon and disruptions in the stable, myelinated speech network of NSs (i.e., as in acquired stuttering). To properly do so would require a more complete understanding than is currently available of how impaired myelogenesis impacts the functional development of non-affected brain regions and fiber tracts.

Increased $\lambda_{\perp}$ in stutterers potential interpretation and limitations

Reductions of FA in neurological diseases are known to arise through several independent mechanisms. For example, significant FA reductions at the voxel level may follow ischemic stroke (Thomalla et al., 2005), adult-onset demyelination syndromes (Vrenken et al., 2006), developmental dysmyelination (Guo et al., 2001), or physical damage to the axons themselves within the fiber tracts (DeBoy et al., 2007). As stated by Budde and colleagues, “anisotropy is an exquisitely sensitive marker of [white matter] pathology”, but anisotropy alone cannot be used to infer the exact origin of this pathology (p. 590) (e.g., damage to axons or loss of their coherent organization versus differences in myelin integrity) (Budde et al., 2008). Therefore, this study sought to extend prior DTI studies of PS by utilizing additional scalar DTI parameters, such as axial ($\lambda_{||}$) and radial diffusivities ($\lambda_{\perp}$), and the trace of the tensor (Tr (D)).

The results of these additional analyses suggest that FA reductions in PDS are largely attributable to an increase in diffusion processes perpendicular to the long axis of WM fibers ($\lambda_{\perp}$). Importantly, this increase in $\lambda_{\perp}$ was detected with no significant differences seen in $\lambda_{\parallel}$. This pattern of reduced FA and increased $\lambda_{\perp}$ is most consistent with the pattern observed in developmental dysmyelination (incomplete CNS myelin formation during development) (Song et al., 2002). Further, studies in animal models (e.g., mice treated with cuprizone to induce demyelination) have demonstrated a close correspondence between histological (e.g., Luxol fast blue-periodic acid-Schiff stain) and DTI measurements (radial diffusivity) of myelination (Song et al., 2005). Finally, the lack of significance in the axial diffusivity measurement suggests these robust FA reductions are not due to a disturbance in the predominant direction of diffusion (e.g., as would be seen in axonal injury (Budde et al., 2008)).

The interpretation of alterations in diffusion anisotropy and radial diffusivity is complex. Any interpretation of changes is complicated by the fact that the exact mechanisms of anisotropy are unknown, a variety of factors might lead to FA reduction, and DTI is inherently a “low-resolution” and “artifact prone” technique (Mori, 2002, p. 392). That said, several potential etiologies of high diffusion anisotropy in DTI have been suggested, including the myelin sheath, the membrane of the axon itself, the geometric arrangement of axons, and the neurofibrils within axons (Beaulieu, 2002; Le Bihan et al., 2001). Experimental evidence testing the contributions of each suggests that the role of myelin is to modulate the degree of anisotropy in tissues where the parallel organization of axons and the axonal membrane itself already ensure relatively high anisotropy (Beaulieu, 2002). This further effect on FA may relate to the fact that the axonal membrane is more permeable to water than myelin, such that in areas of disrupted myelin, reductions in FA are expected (Le Bihan et al., 2001). Relative to the present data, the differences in FA exist in areas with relatively high anisotropy in both groups (see Table 2). As discussed above, the difference between groups then may have to do with the modulation effect of myelin. However, even with an examination of eigenvector alignment (Appendix 2), radial diffusivity changes alone cannot determine that the abnormal component in these individuals is definitely related to myelin content alone (Wheeler-Kingshott and Cercignani, 2009).

Given the potential confounds of both minor eigenvalue comparisons (Wheeler-Kingshott and Cercignani, 2009) and the use of a cross-sectional, case-control design in this study, we acknowledge that dysmyelination is only one interpretation of these results and this should be subjected to further testing. In particular, longitudinal studies of children who stutter with appropriate age-matched controls would be particularly useful in tandem with non-invasive measures more specific for myelination (e.g., magnetic resonance spectroscopy to examine choline peaks (Hausler et al., 2005)).

A longitudinal design might also address whether FA reductions in PSs are a consequence of stuttering behavior and are therefore not developmental in nature. There is a precedent for this hypothesis in the study of other developmental disorders. For example, a study by Klinberg and colleagues (2000) found that individuals with a history of developmental dyslexia had reduced diffusion anisotropy in the bilateral temporoparietal regions and that anisotropy in the region significantly correlated with reading performance. The authors

raised the question of whether the anisotropy changes might follow from impaired reading, as oppose to causing such impairments. For PSs, the strongest evidence that these findings relate to development is that the inter-study agreement between young children and adults who stutter is in relatively good agreement (Figure 2) and there was no relationship here between anisotropy changes in PSs and the mean percentage of syllables stuttered. Even so, the present study cannot provide a definitive answer to this question. To fully answer this question in regard to PSs, future studies will need to utilize a longitudinal study design as has recently been applied to track WM changes following neurological insults (Bendlin et al., 2008). Independent of the underlying mechanism, one benefit of examining inter-study agreement (Figure 2) is that future studies using a longitudinal design will be able to identify robust regions-of-interest to enhance study sensitivity.

Possible relationship of findings to genes recently implicated in stuttering

The current imaging study can only provide new hypotheses in regard to the neuropathological bases of white matter changes in developmental stuttering. However, we note that a developmental dysmyelination hypothesis is not entirely inconsistent with recent genetic evidence. Specifically, Kang and colleagues have identified variations in a region of chromosome 12 (12q23.3) in a small minority of developmental stutterers (Kang et al., 2010). The genes identified in these stutterers are often abnormal in lysosomal storage diseases (mucolipidoses) that are associated with a significant psychomotor delay (Adams and Victor, 1989). Relevant to the present DTI findings, lysosomal storage diseases are associated with damage to the myelin sheath through the engorgement of lysosomes with material that cannot be degraded by dysfunctional lysosomal enzymes (Adams and Victor, 1989). Therefore, lysosomal storage diseases are one of three major categories of developmental dysmyelination (the others being peroxisomal and mitochondrial diseases) (Cheon et al., 2002). It is not clear as yet why developmental stuttering is not associated with more severe neurological deficits and it will be left to future studies to determine how the affected genes impact brain development in PSs, as well as other genes that may be disrupted.

Conclusions

The present study supports earlier conclusions that PSs have reduced FA in the late-myelinating WM tracts of the left hemisphere (Chang et al., 2008; Sommer et al., 2002; Watkins et al., 2008) (Appendix 3). The present study did not find that these reductions were diffuse and bilateral, but did find that the left perisylvian effects included the third division of the SLF (i.e., SLF III), which contains bidirectional connections between inferior parietal and ventral frontal cortices. Using supplemental DTI measures, the diffusion perpendicular to the principal fiber tract orientation, as represented by radial diffusivity, appeared to underlie the FA reductions in PSs. It is therefore likely these findings represent impaired myelogenesis in the WM fiber tracts of the left-hemispheric speech network of PSs. These results also provide evidence that the critical period where brain structural development differs in PSs is within the first few years of postnatal life. The tracts affected here begin myelinating in the first postnatal year in a process that continues well into and past the first decade (Yakovlev and Lecours, 1967). That the postnatal brain maturation of late-

myelinating fiber tracts appears to be the best temporal/ neuroanatomical focus for future studies of brain development in PSs may seem counterintuitive for a neurological disorder with a strong genetic component (Kidd et al., 1981). However, the FA values within all of the WM regions reported here are known to be under “strong genetic control” (Chiang et al., 2009, p. 2220). This suggests that such robust FA reductions might be useful as heritable anatomical endophenotypes (Gottesman and Gould, 2003) to further dissect the genetic bases of developmental stuttering.

Several issues are raised by this study that might be addressed in future studies. First, it is not clear why robust WM findings in PSs are focal and not as diffuse as seen in some disorders of myelogenesis (Hausler et al., 2005). However, this does possibly account for the lack of more pervasive cognitive and motor impairments in PSs compared to well-characterized developmental dysmyelination syndromes (Provenzale et al., 2005). Second, it may be interesting to evaluate pre- and post-treatment FA values within PSs, as experience-dependent, localized FA increases have recently been shown within WM (Scholz et al., 2009). Third, it is not clear how the findings here interact with the persistence versus the untreated (spontaneous) recovery of stuttering in early childhood. This is of particular interest since stuttering can have a rapid onset with modest-to-severe symptomatology, often within the first 36 postnatal months, and in some children will completely resolve within 6 months of onset (Yairi et al., 1993). A logical inference from this would be that stuttering and the untreated, spontaneous recovery from it are directly related to those neurodevelopmental phenomena that have yet to stabilize at this point in postnatal life (i.e., myelination). This argument is bolstered by evidence that FA values within the left perisylvian WM do not differ between children who have spontaneously recovered from stuttering and children who have never stuttered (Chang et al., 2008). Future longitudinal studies of children who stutter, using behavioral and speech measures in tandem with MRI-based measures of myelination (Hausler et al., 2005), should be able to further address this potential link.

Acknowledgments

The authors wish to thank Dr. Anne Cordes Bothe, Ph.D., CCC-SLP and her graduate students at the University of Georgia, Department of Communication Sciences and Special Education, for their assistance in rating percent syllables stuttered and speech naturalness in stuttering participants. We also thank Dr. Jack L. Lancaster, Ph.D., who provided advice on the measurement of subject-specific, voxelwise orientation differences from the group median principle eigenvector. We thank the two anonymous reviewers of the manuscript for their helpful suggestions.

Funding: This work was supported by the National Institute on Deafness and other Communication Disorders of the National Institutes of Health [R01-DC007893 to R.J.I. and P.T.F.; F32-DC009116 to M.D.C.].

APPENDIX 1

The mean percentage of syllables stuttered (% SS) was utilized to avoid issues of multicollinearity with other possible independent variables in the regression model (e.g., % SS telephone, % SS monologue, % SS reading, or maximum value of % SS across any of the three conditions). Specifically, there was a moderate to high correlation between phone and reading task % SS ($r = 0.71$), monologue and reading task % SS ($r = 0.65$), monologue and telephone task % SS ($r = 0.93$), and maximum value of % SS (as used in Cykowski et

al., 2008) and mean value of % SS (r = 0.97). The simultaneous inclusion of these in a single multiple regression model would have decreased the overall power of the model (Bowerman and O'Connell, 1990). Therefore, the mean across three conditions was used as a behavioral covariate so that this hypothesis might be tested while avoiding the potential for biasing the result by sub-selecting among conditions.

APPENDIX 2

The post-hoc validation step was utilized to ensure that minor eigenvalues and their derivatives (radial diffusivity) were suitable for statistical comparisons. This was done by generating a voxelwise group median principal eigenvector (V_1) and computing the angle between the actual V_1 of each subject and the group median. The process was begun by generating a binary mask in standard space for the significant voxels within the superior longitudinal fasciculus (subdivision III). This region-of-interest was chosen as it was closest to the prior finding of Sommer and colleagues (2002) and by virtue of being in perisylvian white matter was possibly susceptible to issues of partial voluming and crossing fiber orientations that might invalidate minor eigenvalue comparisons (Wheeler-Kingshott and Cercignani, 2009). The mask was back projected onto the raw diffusion-weighted data of each subject (using the *tbss_deproject* command of the FMRIB software library). This process first projected significant TBSS skeleton voxels onto the individual subject FA maps that had been nonlinearly registered to the high-resolution FA template (Andersson et al., 2007). The nonlinear registration per subject was then inverted to place the mask of voxels per subject in the space of their original diffusion-weighted data.

The Camino Diffusion MRI Toolkit (Cook et al., 2006) was utilized to extract the three vector components of the principal eigenvector from each subject's diffusion tensor eigensystem. Three images per subject were created ($V1_x$, $V1_y$, $V1_z$) and the voxelwise values of the three vector components were recorded within each subject's back projected mask. Per voxel, a normalized, median principal eigenvector was constructed. The voxelwise angle (in degrees) between individual subject eigenvectors and the group median vector was computed as the arccosine of their dot product.

APPENDIX 3

The term "late-myelinating" as used in the manuscript is intended to convey the relative ordering of myelogenesis in these tracts during early human development and not in reference to the specific subjects under investigation. The labeling of the white matter tracts affected in the present results as late-myelinating is based on neuropathological examinations of these white matter regions for myelin content across a number of postmortem fetal and postnatal samples (Kinney et al., 1988; Yakovlev and Lecours, 1967). It does not refer to the specific subjects under investigation, as the exact timing of myelination would be expected to vary, though within a generally well-defined window (Kinney et al., 1988).

REFERENCES

Adams MR, Hayden P. The ability of stutterers and nonstutterers to initiate and terminate phonation during production of an isolated vowel. J Speech Hear Res. 1976; 19:290–296. [PubMed: 979203]

Andersson JLR, Jenkinson M, Smith S. Non-linear registration. FMRIB technical report TR07JA2. 2007Found at www.fmrib.ox.ac.uk/analysis/techrep

Armstrong E, Schleicher A, Omran H, Curtis M, Zilles K. The ontogeny of human gyrification. Cereb Cortex. 1995; 5:56–63. [PubMed: 7719130]

Basser PJ, Jones DK. Diffusion-tensor MRI: theory, experimental design and data analysis - a technical review. NMR Biomed. 2002; 15:456–467. [PubMed: 12489095]

Beal DS, Gracco VL, Lafaille SJ, De Nil LF. Voxel-based morphometry of auditory and speech-related cortex in stutterers. Neuroreport. 2007; 18:1257–1260. [PubMed: 17632278]

Bendlin BB, Ries ML, Lazar M, Alexander AL, Dempsey RJ, Rowley HA, Sherman JE, Johnson SC. Longitudinal changes in patients with traumatic brain injury assessed with diffusion-tensor and volumetric imaging. Neuroimage. 2008; 42:503–514. [PubMed: 18556217]

Benson, DF.; Ardila, A. Aphasia: a clinical perspective. New York: Oxford University Press; 1996.

Bloodstein, O.; Ratner, NB. A handbook on stuttering. 6th ed.. Clifton Park, NY: Thomson/Delmar Learning; 2008.

Bowerman, BL.; O'Connell, RT. Linear statistical models: an applied approach. Boston: PWS-Kent Pub. Co; 1990.

Braun AR, Varga M, Stager S, Schulz G, Selbie S, Maisog JM, Carson RE, Ludlow CL. Altered patterns of cerebral activity during speech and language production in developmental stuttering. An H2(15)O positron emission tomography study. Brain. 1997; 120(Pt 5):761–784. [PubMed: 9183248]

Budde MD, Kim JH, Liang HF, Russell JH, Cross AH, Song SK. Axonal injury detected by in vivo diffusion tensor imaging correlates with neurological disability in a mouse model of multiple sclerosis. NMR Biomed. 2008; 21:589–597. [PubMed: 18041806]

Chang LC, Jones DK, Pierpaoli C. RESTORE: robust estimation of tensors by outlier rejection. Magn Reson Med. 2005; 53:1088–1095. [PubMed: 15844157]

Chang SE, Erickson KI, Ambrose NG, Hasegawa-Johnson MA, Ludlow CL. Brain anatomy differences in childhood stuttering. Neuroimage. 2008; 39:1333–1344. [PubMed: 18023366]

Chang SE, Kenney MK, Loucks TM, Ludlow CL. Brain activation abnormalities during speech and non-speech in stuttering speakers. Neuroimage. 2009; 46:201–212. [PubMed: 19401143]

Cheon JE, Kim IO, Hwang YS, Kim KJ, Wang KC, Cho BK, et al. Leukodystrophy in children: a pictorial review of MR imaging features. Radiographics. 2002; 22:461–476. [PubMed: 12006681]

Chiang MC, Barysheva M, Shattuck DW, Lee AD, Madsen SK, Avedissian C, Klunder AD, Toga AW, McMahon KL, de Zubicaray GI, Wright MJ, Srivastava A, Balov N, Thompson PM. Genetics of brain fiber architecture and intellectual performance. J Neurosci. 2009; 29:2212–2224. [PubMed: 19228974]

Conture EG, McCall GN, Brewer DW. Laryngeal behavior during stuttering. J Speech Hear Res. 1977; 20:661–668. [PubMed: 604680]

Cook, PA.; Bai, Y.; Nedjati-Gilani, S.; Seunarine, KK.; Hall, MG.; Parker, GJ.; Alexander, DC. Camino: Open-Source Diffusion-MRI Reconstruction and Processing. 14th Scientific Meeting of the International Society for Magnetic Resonance in Medicine; Seattle, Washington, USA. 2006.

Cykowski MD, Kochunov PV, Ingham RJ, Ingham JC, Mangin JF, Riviere D, Lancaster JL, Fox PT. Perisylvian sulcal morphology and cerebral asymmetry patterns in adults who stutter. Cereb Cortex. 2008; 18:571–583. [PubMed: 17584852]

De Nil LF, Kroll RM, Kapur S, Houle S. A positron emission tomography study of silent and oral single word reading in stuttering and nonstuttering adults. J Speech Lang Hear Res. 2000; 43:1038–1053. [PubMed: 11386470]

DeBoy CA, Zhang J, Dike S, Shats I, Jones M, Reich DS, Mori S, Nguyen T, Rothstein B, Miller RH, Griffin JT, Kerr DA, Calabresi PA. High resolution diffusion tensor imaging of axonal damage in

focal inflammatory and demyelinating lesions in rat spinal cord. Brain. 2007; 130:2199–2210. [PubMed: 17557778]

Foundas AL, Bollich AM, Corey DM, Hurley M, Heilman KM. Anomalous anatomy of speech-language areas in adults with persistent developmental stuttering. Neurology. 2001; 57:207–215. [PubMed: 11468304]

Foundas AL, Corey DM, Angeles V, Bollich AM, Crabtree-Hartman E, Heilman KM. Atypical cerebral laterality in adults with persistent developmental stuttering. Neurology. 2003; 61:1378–1385. [PubMed: 14638959]

Fox PT, Ingham RJ, Ingham JC, Hirsch TB, Downs JH, Martin C, Jerabek P, Glass T, Lancaster JL. A PET study of the neural systems of stuttering. Nature. 1996; 382:158–161. [PubMed: 8700204]

Galaburda AM, LeMay M, Kemper TL, Geschwind N. Right-left asymmetrics in the brain. Science. 1978; 199:852–856. [PubMed: 341314]

Gottesman II, Gould TD. The endophenotype concept in psychiatry: etymology and strategic intentions. Am J Psychiatry. 2003; 160:636–645. [PubMed: 12668349]

Greiner JR, Fitzgerald HE, Cooke PA. Speech Fluency and Hand Performance on a Sequential Tapping Task in Left-Handed and Right-Handed Stutterers and Non-Stutterers. Journal of Fluency Disorders. 1986; 11:55–69.

Guenther FH, Ghosh SS, Tourville JA. Neural modeling and imaging of the cortical interactions underlying syllable production. Brain and Language. 2006; 96:280–301. [PubMed: 16040108]

Guo AC, Petrella JR, Kurtzberg J, Provenzale JM. Evaluation of white matter anisotropy in Krabbe disease with diffusion tensor MR imaging: initial experience. Radiology. 2001; 218:809–815. [PubMed: 11230660]

Harsan LA, Poulet P, Guignard B, Parizel N, Skoff RP, Ghandour MS. Astrocytic hypertrophy in dysmyelination influences the diffusion anisotropy of white matter. J Neurosci Res. 2007; 85:935–944. [PubMed: 17278151]

Hausler M, Anhuf D, Schuler H, Ramaekers VT, Thron A, Zerres K, Moller-Hartmann W. White-matter disease in 18q deletion (18q-) syndrome: magnetic resonance spectroscopy indicates demyelination or increased myelin turnover rather than dysmyelination. Neuroradiology. 2005; 47:83–86. [PubMed: 15645149]

Hickok G, Poeppel D. The cortical organization of speech processing. Nat Rev Neurosci. 2007; 8:393–402. [PubMed: 17431404]

Santa Barbara, Santa Barbara: University of California; 1999. Stuttering Measurement System (SMS). [Software, manual, and training materials]

Ingham, RJ.; Cykowski, MD.; Ingham, J.; Fox, PT. Neuroimaging contributions to developmental stuttering theory and treatment. In: Ingham, RJ., editor. Neuroimaging in communication sciences and disorders. San Diego: Plural Publishing; 2007. p. 53-85.

Ingham RJ, Fox PT, Costello Ingham J, Zamarripa F. Is overt stuttered speech a prerequisite for the neural activations associated with chronic developmental stuttering? Brain Lang. 2000; 75:163–194. [PubMed: 11049665]

Jancke L, Hanggi J, Steinmetz H. Morphological brain differences between adult stutterers and non-stutterers. BMC Neurol. 2004; 4:23. [PubMed: 15588309]

Jenkinson M, Bannister P, Brady M, Smith S. Improved optimization for the robust and accurate linear registration and motion correction of brain images. Neuroimage. 2002; 17:825–841. [PubMed: 12377157]

Jones DK, Horsfield MA, Simmons A. Optimal strategies for measuring diffusion in anisotropic systems by magnetic resonance imaging. Magn Reson Med. 1999; 42:515–525. [PubMed: 10467296]

Kang C, Riazuddin S, Mundorff J, Krasnewich D, Friedman P, Mullikin JC, Drayna D. Mutations in the Lysosomal Enzyme-Targeting Pathway and Persistent Stuttering. N Engl J Med. 2010 2010 [in press].

Kell CA, Neumann K, von Kriegstein K, Posenenske C, von Gudenberg AW, Euler H, Giraud AL. How the brain repairs stuttering. Brain. 2009; 132:2747–2760. [PubMed: 19710179]

Kidd KK, Heimbuch RC, Records MA. Vertical transmission of susceptibility to stuttering with sex-modified expression. Proc Natl Acad Sci U S A. 1981; 78:606–610. [PubMed: 6941261]

Kinney HC, Brody BA, Kloman AS, Gilles FH. Sequence of central nervous system myelination in human infancy. II. Patterns of myelination in autopsied infants. J Neuropathol Exp Neurol. 1988; 47:217–234. [PubMed: 3367155]

Klinberg T, Hedehus M, Temple E, Salz T, Gabrieli JDE, Moseley ME, Poldrack RA. Microstructure of Temporo-Parietal White Matter as a Basis for Reading Ability: Evidence from Diffusion Tensor Magnetic Resonance Imaging. Neuron. 2000; 25:493–500. [PubMed: 10719902]

Kochunov P, Thompson PM, Lancaster JL, Bartzokis G, Smith S, Coyle T, et al. Relationship between white matter fractional anisotropy and other indices of cerebral health in normal aging: tract-based spatial statistics study of aging. Neuroimage. 2007; 35:478–487. [PubMed: 17292629]

Kochunov P, Coyle T, Lancaster J, Robin DA, Hardies J, Kochunov V, et al. Processing speed is correlated with cerebral health markers in the frontal lobes as quantified by neuroimaging. Neuroimage. 2010; 49:1190–1199. [PubMed: 19796691]

Le Bihan D, Mangin JF, Poupon C, Clark CA, Pappata S, Molko N, Chabriat H. Diffusion tensor imaging: Concepts and applications. Journal of Magnetic Resonance Imaging. 2001; 13:534–546. [PubMed: 11276097]

Ludlow CL, Loucks T. Stuttering: a dynamic motor control disorder. J Fluency Disord. 2003; 28:273–295. quiz 295. [PubMed: 14643066]

Makris N, Kennedy DN, McInerney S, Sorensen AG, Wang R, Caviness VS Jr, Pandya DN. Segmentation of subcomponents within the superior longitudinal fascicle in humans: a quantitative, in vivo, DT-MRI study. Cereb Cortex. 2005; 15:854–869. [PubMed: 15590909]

Max L, Caruso AJ, Gracco VL. Kinematic analyses of speech, orofacial nonspeech, and finger movements in stuttering and nonstuttering adults. J Speech Lang Hear Res. 2003; 46:215–232. [PubMed: 12647900]

Mori, S. Principles, Methods, and Applications of Diffusion Tensor Imaging. In: Toga, A.; Mazziotta, J., editors. Brain Mapping: The Methods. San Diego: Academic Press; 2002. p. 379-397.

Mori S, Oishi K, Jiang H, Jiang L, Li X, Akhter K, Hua K, Faria AV, Mahmood A, Woods R, Toga AW, Pike GB, Neto PR, Evans A, Zhang J, Huang H, Miller MI, van Zijl P, Mazziotta J. Stereotaxic white matter atlas based on diffusion tensor imaging in an ICBM template. Neuroimage. 2008; 40:570–582. [PubMed: 18255316]

Nichols TE, Holmes AP. Nonparametric permutation tests for functional neuroimaging: A primer with examples. Hum Brain Mapp. 2002; 15:1–25. [PubMed: 11747097]

Oldfield RC. The assessment and analysis of handedness: the Edinburgh inventory. Neuropsychologia. 1971; 9:97–113. [PubMed: 5146491]

Orton ST. Studies in stuttering. Archives of Neurology Psychiatry. 1927; 18:671–672.

Provenzale JM, Escolar M, Kurtzberg J. Quantitative analysis of diffusion tensor imaging data in serial assessment of Krabbe disease. Ann N Y Acad Sci. 2005; 1064:220–229. [PubMed: 16394159]

Schmahmann, JD.; Pandya, DN. Fiber pathways of the brain. New York: Oxford University Press, Oxford; 2006.

Scholz J, Klein MC, Behrens TE, Johansen-Berh H. Training induces changes in white-matter architecture. Nature Neuroscience. 2009; 12:1370–1371.

Sidman RL, Rakic P. Neuronal migration, with special reference to developing human brain: a review. Brain Res. 1973; 62:1–35. [PubMed: 4203033]

Smith SM, Jenkinson M, Johansen-Berg H, Rueckert D, Nichols TE, Mackay CE, Watkins KE, Ciccarelli O, Cader MZ, Matthews PM, Behrens TE. Tract-based spatial statistics: voxelwise analysis of multi-subject diffusion data. Neuroimage. 2006; 31:1487–1505. [PubMed: 16624579]

Smith SM, Jenkinson M, Woolrich MW, Beckmann CF, Behrens TE, Johansen-Berg H, Bannister PR, De Luca M, Drobnjak I, Flitney DE, Niazy RK, Saunders J, Vickers J, Zhang Y, De Stefano N, Brady JM, Matthews PM. Advances in functional and structural MR image analysis and implementation as FSL. Neuroimage. 2004; 23(Suppl 1):S208–S219. [PubMed: 15501092]

Smith SM, Nichols TE. Threshold-free cluster enhancement: addressing problems of smoothing, threshold dependence and localisation in cluster inference. Neuroimage. 2009; 44:83–98. [PubMed: 18501637]

Sommer M, Koch MA, Paulus W, Weiller C, Buchel C. Disconnection of speech-relevant brain areas in persistent developmental stuttering. Lancet. 2002; 360:380–383. [PubMed: 12241779]

Sommer M, Knappmeyer K, Hunter EJ, Gudenberg AW, Neef N, Paulus W. Normal interhemispheric inhibition in persistent developmental stuttering. Mov Disord. 2009; 24:769–773. [PubMed: 19224611]

Song SK, Sun SW, Ramsbottom MJ, Chang C, Russell J, Cross AH. Dysmyelination revealed through MRI as increased radial (but unchanged axial) diffusion of water. Neuroimage. 2002; 17:1429–1436. [PubMed: 12414282]

Song SK, Yoshino J, Le TQ, Lin SJ, Sun SW, Cross AH, Armstrong RC. Demyelination increases radial diffusivity in corpus callosum of mouse brain. Neuroimage. 2005; 26:132–140. [PubMed: 15862213]

Stager SV, Jeffries KJ, Braun AR. Common features of fluency-evoking conditions studied in stuttering subjects and controls: an H(2)15O PET study. J Fluency Disord. 2003; 28:319–335. quiz 336. [PubMed: 14643068]

Thomalla G, Glauche V, Weiller C, Rother J. Time course of wallerian degeneration after ischaemic stroke revealed by diffusion tensor imaging. J Neurol Neurosurg Psychiatry. 2005; 76:266–268. [PubMed: 15654048]

Vrenken H, Pouwels PJ, Geurts JJ, Knol DL, Polman CH, Barkhof F, Castelijns JA. Altered diffusion tensor in multiple sclerosis normal-appearing brain tissue: cortical diffusion changes seem related to clinical deterioration. J Magn Reson Imaging. 2006; 23:628–636. [PubMed: 16565955]

Watkins KE, Smith SM, Davis S, Howell P. Structural and functional abnormalities of the motor system in developmental stuttering. Brain. 2008; 131:50–59. [PubMed: 17928317]

Webster, WG. Hurried hands and tangled tongues. In: Boberg, E., editor. Neuropsychology of stuttering. Edmonton: The University of Alberta Press; 1993. p. 73-127.

Wingate ME. A Standard Definition of Stuttering. J Speech Hear Disord. 1964; 29:484–489. [PubMed: 14257050]

Wu JC, Maguire G, Riley G, Fallon J, Lacasse L, Chin S, Klein E, Tang C, Cadwell S, Lottenberg S. A Positron Emission Tomography [F-18] Deoxyglucose Study of Developmental Stuttering. Neuroreport. 1995; 6:501–505. [PubMed: 7766852]

Yairi E, Ambrose NG, Niermann R. The early months of stuttering: a developmental study. J Speech Hear Res. 1993; 36:521–528. [PubMed: 8331909]

Yakovlev, P.; Lecours, A. The myelogenetic cycles of regional maturation of the brain. In: Minkowski, A., editor. Regional Development of the Brain in Early Life. Oxford: Blackwell; 1967. p. 3-70.

Yates AJ. Recent empirical and theoretical approaches to the experimental manipulation of speech in normal subjects and in stammerers. Behaviour Research and Therapy. 1963; 1:95–119. [PubMed: 14153346]

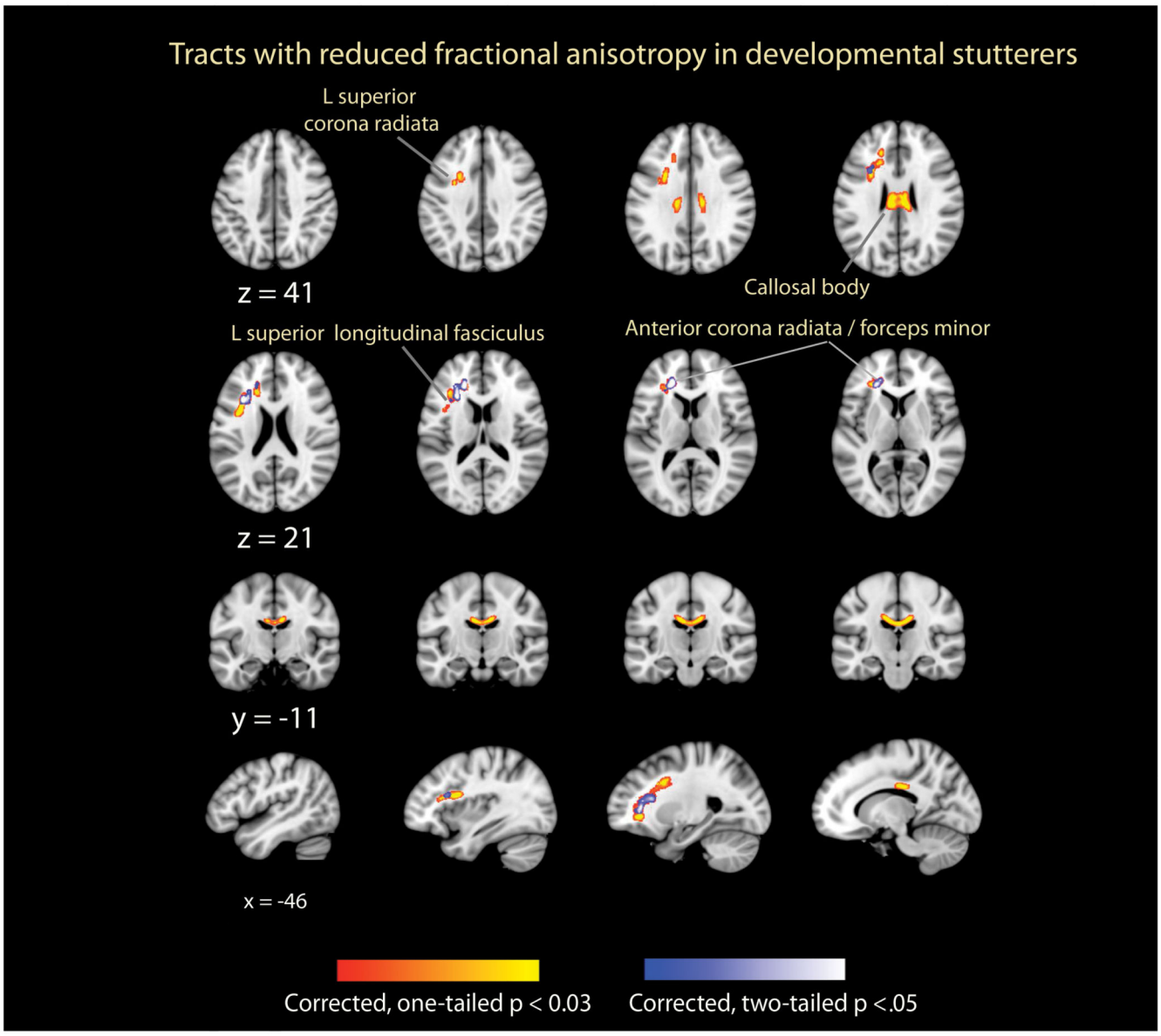

Figure 1.

Axial (rows 1 and 2), coronal (row 3), and sagittal (row 4) views of fiber tracts where fractional anisotropy (FA) was significantly reduced in PSs relative to normally fluent speakers NSs. The axial images are displayed in neurological format (the left of the brain is on left-hand side) using the Montreal Neurological Institute (MNI) coordinate system. The affected regions are displayed using both a red-to-yellow overlay (corrected, one-tailed results) and blue-to-white overlay (corrected, two-tailed results). For clarity, these affected regions have been “thickened” for display purposes using the using tools in the FMRIB software library (FSL). Axial slices are separated by 5 mm, coronal slices by 3 mm, and sagittal slices by 11 mm.

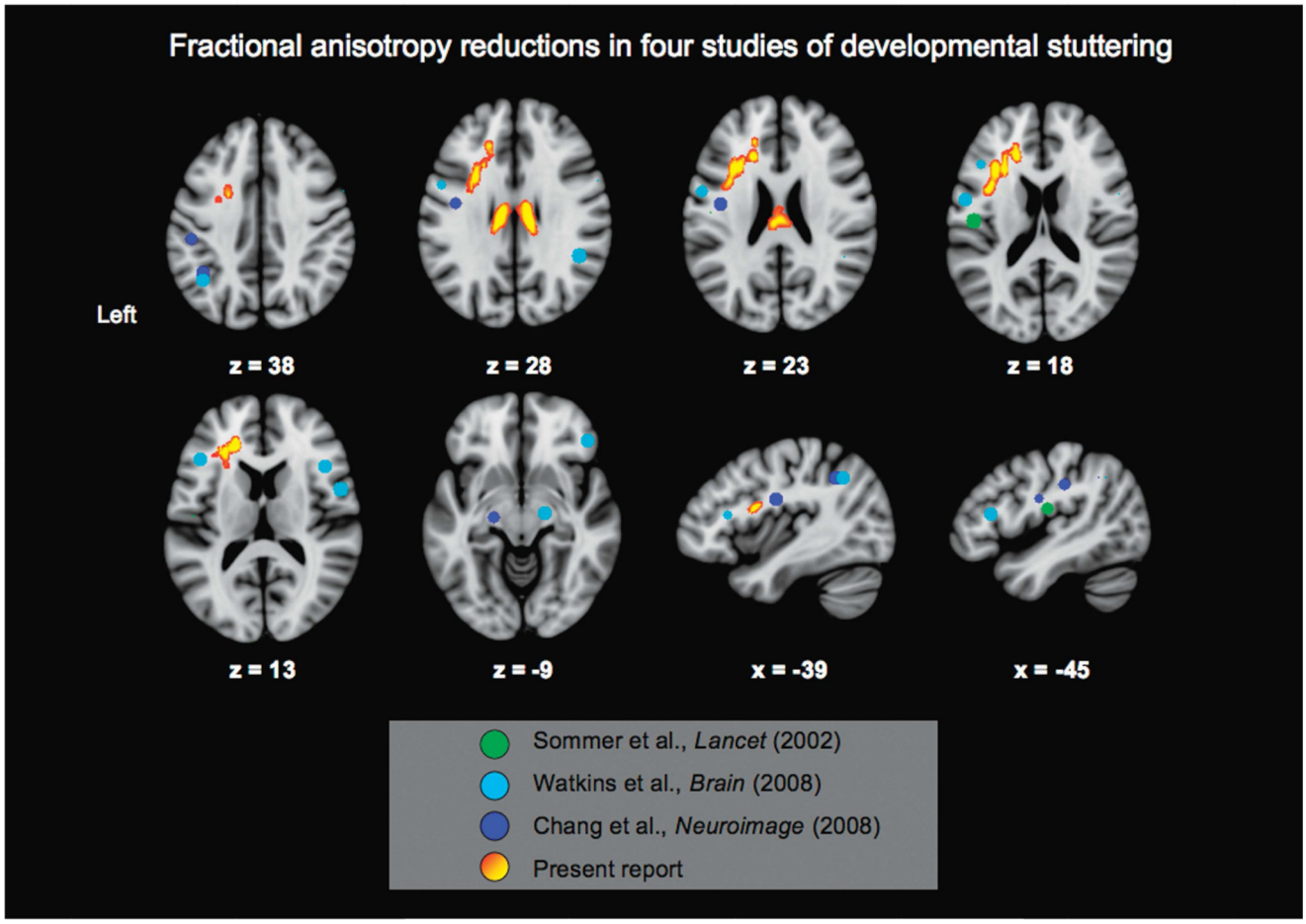

Figure 2.

Significant FA reductions in PSs as compared to NSs across four studies of developmental stuttering. The significant results of the present study are overlain as thickened voxels (see Figure 1 and caption). For the remaining three studies, the peak coordinates reported per study were used to generate spherical regions-of-interest and are color-coded with a legend at the bottom of the figure.

Table 1

Characteristics of PSs and NSs study participants.

	PSs mean (N = 13)	NSs mean (N = 14)
Age	31.0 (SD = 13.72)	30.4 (SD = 14.83)
EHI[1]	88.4 (12.91)	84.3 (16.03)
Education (years)	15.8 (2.39)	16.5 (2.15)
Percentage syllables stuttered[2]	4.2 (3.39)	N/A[3]

[1] The Edinburgh handedness inventory (EHI) score (Oldfield, 1971). Higher scores indicate greater right-hand dominance.

[2] The mean percentage of syllables stuttered across 3-minute oral reading, phone, and monologue assessments.

[3] The speech of control speakers was also examined using 3-minute oral reading, phone, and monologue assessments. These audiovisual recordings were reviewed by two independent sets of judges, blind to subject grouping and expert in the evaluation of PSs. Both sets of judges agreed that all control subjects were fluent speakers who did not have any events of stuttered speech.

Table 2

Mean DTI parameters by tract in PSs and NSs.

Fiber tract cluster 1: **Left anterior corona radiata[1] (*centroid*), Left forceps minor of corpus callosum (*anterior extension*) Left superior longitudinal fasciculus, subdivision III (*posterior extension*)**							
Size[2]	**x[3]**	**y**	**z**	**Parameter[4]**	**NSs**	**PSs**	**P-value[6]**
1339	−25/ −24.7	25/ 25	17/ 14.4	*FA*	0.50 (0.030)	0.45 (0.025)	-
				$\lambda_{\|\|}$[5]	1.20 (0.054)	1.19 (0.049)	0.488
				$\lambda_{\perp}$[5]	0.54 (0.033)	0.60 (0.028)	≤ ***0.001***[7]
				Tr (D)[5]	2.28 (0.093)	2.38 (0.084)	0.012
Fiber tract cluster 2: Body of corpus callosum[1] (*centroid*)							
Size[2]	**x[3]**	**y**	**z**	**Parameter[4]**	**NSs**	**PSs**	**P-value[5]**
410	0/ 0	−19/ −17.2	27/ 25.7	*FA*	0.78 (0.044)	0.71 (0.045)	-
				$\lambda_{\|\|}$	1.87 (0.075)	1.85 (0.070)	0.28
				$\lambda_{\perp}$	0.36 (0.078)	0.48 (0.069)	≤ ***0.001***
				Tr (D)	2.60 (0.192)	2.80 (0.145)	***0.001***

[1] Fiber tract labels from Makris et al. (2004), Mori et al. (2005), Mori et al. (2008).

[2] Size represents both number of voxels and volume (1 mm isotropic resolution).

[3] Centroid coordinates for affected tracts given in the following convention: MNI (FSL)/ Talairach.

[4] See text for explanation of DTI parameters.

[5] Value × 10^{-3} mm^2/s.

[6] P-value from posthoc Mann-Whitney U test. Whole brain FA analyses are presented in Figure 1.

[7] Bold type indicates significant posthoc comparisons below the corrected p-value ($p \leq 8.33 \times 10^{-3}$).